Impurity states in the one-dimensional Bose gas

Volodymyr Pastukhov*
Department for Theoretical Physics, Ivan Franko National University of Lviv, 12 Drahomanov Street, Lviv-5, 79005 Ukraine
(Received 10 July 2017; published 25 October 2017)

The detailed study of the low-energy spectrum for a mobile impurity in the one-dimensional bosonic environment is performed. Particularly we have considered only two analytically accessible limits, namely, the case of an impurity immersed in a dilute Bose gas where one can use many-body perturbative techniques for low-dimensional bosonic systems and the case of the Tonks-Girardeau gas for which the usual fermionic diagrammatic expansion up to the second order is applied.

DOI: 10.1103/PhysRevA.96.043625

I. INTRODUCTION

The behavior of impurity in the various media is a cornerstone problem for the understanding of numerous phenomena in the condensed-matter physics including the Kondo effect, Anderson localization, etc. Recently, great attention from theorists [1–12] has been paid to the analysis of mobile impurity properties in the Bose gas. Such a renascence of the old problem well studied in the context of a single ^{3}He atom immersed in liquid ^{4}He (see, for instance, Refs. [13–16] and references there) is stimulated by the success of the experimental techniques [17,18] where the possibility to control a small amount of impurity particles strongly coupled to the bosonic bath is demonstrated.

A very interesting platform for the theoretical research in the Bose polaron problem is the case of one-dimensional environments [19–26]. It is well known that due to highly nontrivial physics in the one spatial dimension [27,28] these systems possess unexpected behavior which very often obstructs their analysis. In some limiting cases, however, they admit analytical treatment [29] or even the existence of exact solutions [30–34]. There is also an experimental realization of the one-dimensional Bose polaron [35] where a minority of ^{41}K atoms immersed in the ^{87}Rb medium was observed during expansion and the prediction for the impurity effective mass within Feynman's framework was given. Essentially exact recent Monte Carlo simulations [36] revealed the impact of the considerably strong phonon-mediated interaction on the properties of a one-dimensional Bose polaron, and to describe the system properly one needs to go beyond [37] the Fröhlich model in this case.

II. FORMULATION

We study the properties of a single impurity atom immersed in the Lieb-Liniger gas. It is assumed that the impurity interacts with bath particles via a contact potential and by appropriately choosing a sign of the coupling constant we reproduce both repulsive and attractive Bose polarons. In order to take advantage of the many-body perturbation theory we consider the Bose-Fermi mixture consisting of a very dilute spinless (spin-polarized) Fermi gas immersed in the bosonic medium. The described model is characterized by the following Hamiltonian:

$$H = H_0 + H_B + H_{\rm int}, \tag{2.1}$$

where H_0 describes the ideal Fermi gas (m_i is the mass of the impurity particle),

$$H_0 = -\frac{\hbar^2}{2m_i}\int_0^L dx\, \psi^+(x)\partial_x^2\psi(x). \tag{2.2}$$

Here fermionic creation $\psi^+(x)$ and annihilation $\psi(x)$ field operators which refer to the impurity states and satisfy usual anticommutating relations $\{\psi(x),\psi^+(x')\} = \delta(x - x')$, $\{\psi(x),\psi(x')\} = 0$. The second term in Eq. (2.1) is the Hamiltonian of Bose particles of mass m interacting with the δ-like repulsive potential,

$$H_B = -\frac{\hbar^2}{2m}\int_0^L dx\, \phi^+(x)\partial_x^2\phi(x) + \frac{g}{2}\int_0^L dx[\phi^+(x)]^2[\phi(x)]^2, \tag{2.3}$$

where we have introduced field operators $\phi^+(x)$,$\phi(x)$ of the Bose type. Finally, the last term of H takes into account the interaction of Bose-Fermi subsystems,

$$H_{\rm int} = \tilde{g}\int_0^L dx\, \psi^+(x)\psi(x)\phi^+(x)\phi(x). \tag{2.4}$$

It is well known that the formulated model (2.1) can be solved exactly within the Bethe ansatz only when $m_i = m$, otherwise some approximate calculational schemes should be applied. But this equal-mass limit is a good benchmark for any perturbative approach. In the following sections we will consider two opposite models of environments given by Hamiltonian (2.3), namely, a dilute Bose gas [Bose-Einstein condensate (BEC)] $g \to 0$ and a case of the Tonks-Girardeau (TG) limit $g \to \infty$.

A. Impurity in the dilute Bose gas

For the low-dimensional systems $D \leqslant 2$ where the condensate does not exist at finite temperatures it is convenient to introduce the phase-density representation [27,38,39] for the bosonic operators: $\phi(x) = e^{i\varphi(x)}\sqrt{n(x)}$, $\phi^+(x) = \sqrt{n(x)}e^{-i\varphi(x)}$ with commutator $[n(x),\varphi(x')] = i\delta(x - x')$ for the phase $\varphi(x)$ and density $n(x) = \phi^+(x)\phi(x)$ fields. Imposing periodic boundary conditions $n(x + L) = n(x)$, $\phi(x + L) = \phi(x)$ with large "volume" L and making use of

*volodyapastukhov@gmail.com

the Fourier transform $n(x) = n + \frac{1}{\sqrt{L}}\sum_{k\neq 0} e^{ikx} n_k$, $\varphi(x) = \frac{1}{\sqrt{L}}\sum_{k\neq 0} e^{-ikx}\varphi_k$, where $n = N/L$ is the equilibrium density of the Bose system; substituting $\varphi(x)$,$n(x)$ in Eq. (2.3) and then performing canonical transformations $b_k = i\sqrt{n/\alpha_k}\,\varphi_{-k} + \frac{1}{2}\sqrt{\alpha_k/n}n_k$, $b_k^+ = -i\sqrt{n/\alpha_k}\varphi_k + \frac{1}{2}\sqrt{\alpha_k/n}n_{-k}$ (note that $[b_k,b_q^+] = \delta_{k,q}$ and $[b_k,b_q] = 0$) that diagonalize the quadratic part of the Hamiltonian H_B we finally obtain

$$H_B = E_0 + \sum_{k\neq 0} E_k b_k^+ b_k + \Delta H_B, \tag{2.5}$$

$$\Delta H_B = \frac{1}{3!\sqrt{N}}\sum_{k+q+s=0} D_{bbb}(k,q,s) b_k b_q b_s + \text{H.c.} + \frac{1}{2\sqrt{N}}\sum_{k,q\neq 0} D_{b^+bb}(k+q|k,q) b_{k+q}^+ b_k b_q + \text{H.c.}, \tag{2.6}$$

where E_0 and E_k are the Bogoliubov ground-state energy and the quasiparticle spectrum, respectively. Introducing bosonic free-particle dispersion $\varepsilon_k = \hbar^2 k^2/2m$ one may show that the above-mentioned requirement of diagonalization fixes parameter $\alpha_k = E_k/\varepsilon_k$. It should be noted that in ΔH_B the only relevant terms for our two-loop calculations are presented. The functions,

$$\left.\begin{matrix} D_{bbb}(k,q,s) \\ D_{b^+bb}(s|k,q) \end{matrix}\right\} = \frac{\hbar^2}{4m\sqrt{\alpha_k\alpha_q\alpha_s}}[kq(\alpha_k\alpha_q + 1) + ks(\alpha_k\alpha_s \pm 1) + qs(\alpha_q\alpha_s \pm 1)] \tag{2.7}$$

describe the simplest scattering processes of the elementary excitations. In the same fashion we rewrite the third term of the Hamiltonian,

$$H_{\text{int}} = n\tilde{g}\sum_p \psi_p^+\psi_p + \frac{1}{\sqrt{L}}\sum_{p;k\neq 0} \tilde{g}\sqrt{n/\alpha_k}(b_k^+ + b_{-k})\psi_p^+\psi_{p+k}, \tag{2.8}$$

where operators ψ_p^+ and ψ_p are the Fourier transforms of $\psi^+(x)$ and $\psi(x)$, respectively. Although we are going to discuss the ground-state properties of the impurity atom immersed in a Bose gas, for the further analysis we adopt the field-theoretical formulation at finite temperatures [40]. The exact single-particle Green's function of the fermions in the four-momentum space is given by

$$G_i^{-1}(P) = i\nu_p - \xi_i(p) - \Sigma(P), \tag{2.9}$$

where $P = (\nu_p, p)$ (ν_p is the fermionic Matsubara frequency); $\xi_i(p) = \hbar^2 p^2/2m_i - \tilde{\mu}_i$ where the chemical potential of the Fermi gas $\tilde{\mu}_i = \mu_i - n\tilde{g}$ shifted due to interaction with the Bose subsystem ensures the particle number conservation. The exact self-energy of the impurity is given by two skeleton diagrams depicted in Fig. 1,

$$\Sigma(P) = \frac{-\tilde{g}}{L\beta}\sum_K \sqrt{\frac{n}{\alpha_k}}\Gamma_{b^+}(P-K,P)G_B(K)G_i(P-K) - \frac{\tilde{g}}{L\beta}\sum_K \sqrt{\frac{n}{\alpha_k}}\Gamma_b(P+K,P)G_B(K)G_i(K+P), \tag{2.10}$$

FIG. 1. Exact diagrammatic representation of self-energy $\Sigma(P)$ in the weakly interacting Bose gas. The bold solid line represents the exact one-particle fermionic Green's function. The dashed line is the bosonic propagator in the Bogoliubov approximation. The dots stand for the zero-order (light) and the exact (black) vertices, respectively.

where we already have taken into account the diluteness of the Bose gas, i.e., neglected the self-energy corrections to the Green's-function $G_B(K)$ of Bogoliubov's quasiparticles.

This is formally an exact equation that determines the impurity Green's-function self-consistently. Technically this program for a given approximation of the boson-fermion vertices $\Gamma_{b^+}(P-K,P)$ and $\Gamma_b(P+K,P)$ is very hard for practical realization, therefore, in the following we will use perturbation theory. The appropriative expansion parameter is the coupling constant $\tilde{g}$ that characterizes the intensity of the two-particle Bose-Fermi interaction which we accept to be small in our calculations. Following this ideology one readily mentions that the correction of order $\tilde{g}^2$ to the self-energy $\Sigma^{(1)}(P)$ is fully determined by the first diagram in Fig. 1 with $\Gamma_{b^+}(P-K,P) \to \tilde{g}\sqrt{n/\alpha_k}$ and $G_i(P) \to 1/[i\nu_p - \xi_i(p)]$. In this approximation the second diagram provides the nonzero contribution only at finite temperatures. On the two-loop level which particularly contains $\tilde{g}^3$ and $\tilde{g}^4$ terms of the impurity self-energy the situation is more complicated because now we have to take into account six diagrams (see Fig. 2) for each vertex $\Gamma_b(P+K,P)$,$\Gamma_{b^+}(P-K,P)$ and to use the impurity Green's function complicated with the first-order correction $G_i(P) = 1/[i\nu_p - \xi_i(p)] + \Sigma^{(1)}(P)/[i\nu_p - \xi_i(p)]^2$ in the first diagram in Fig. 1. The details of these calculations as well as the explicit formula for the self-energy up to the second order of a perturbation theory can be found in Appendix A. Finally, it should be noted that the second-order formula for the self-energy obtained in this section can be applied to the Bose polaron problem in higher dimensions, for instance, in the three-dimensional case it reproduces the results of Ref. [6].

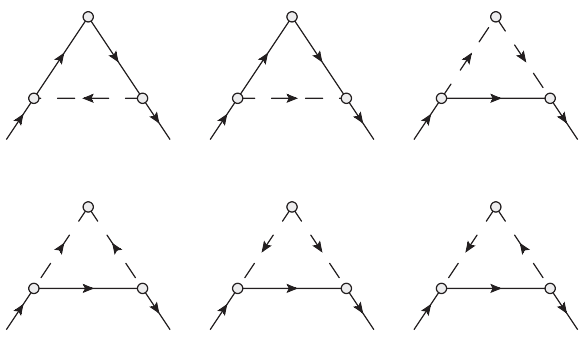

FIG. 2. One-loop diagrams contributing to the vertices $\Gamma_b(P+K,P)$,$\Gamma_{b^+}(P-K,P)$.

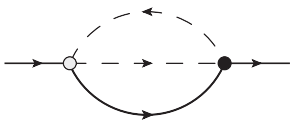

FIG. 3. The self-energy of the impurity atom immersed in the TG gas. Here the black dot denotes the exact vertex $T(Q-K;P+K|P;Q)$, whereas the light dot stands for the Fourier-transform $\tilde{g}$ of a bare interaction potential.

B. The Tonks-Girardeau limit

Another interesting limit where the perturbative calculations may be performed analytically is the case of the impurity immersed in the Bose gas with infinite ($g\to\infty$) interparticle repulsion. In this limit the bosons become nonpenetrable and operators $\phi^+(x)$,$\phi(x)$ by means of the Jordan-Wigner transformation can be mapped onto fermionic creation and annihilation field operators [27]. This transformation leaves the first term of Hamiltonian (2.3) unchanged and nullifies the second one. Therefore in the following we have to consider the properties of the one-dimensional Fermi-Fermi mixture with unequal masses of two sorts of particles. The interaction is assumed to be switched on only between atoms of different species. The appropriate grand-canonical Hamiltonian $H'=H-\sum_p\{\mu_i\psi_p^+\psi_p+\mu\phi_p^+\phi_p\}$ reads

$$H'=\sum_p\{\xi_i(p)\psi_p^+\psi_p+\xi_p\phi_p^+\phi_p\}+\frac{1}{L}\sum_{p,q,k}\tilde{g}\psi_p^+\phi_q^+\phi_{q+k}\psi_{p-k}, \tag{2.11}$$

where $\xi_p=\varepsilon_p-\mu$ with $\mu=\hbar^2p_0^2/2m$ ($p_0=\pi n$) being the chemical potential of the Bose gas in the TG limit and we now have to treat ϕ_p^+ and ϕ_p as Fermi creation and annihilation operators, respectively. Then the impurity self-energy in the TG gas is (see Fig. 3)

$$\Sigma(P)=-\frac{\tilde{g}}{(L\beta)^2}\sum_{K,Q}T(Q-K;P+K|P;Q)\times G_0(Q)G_0(Q-K)G_i(P+K). \tag{2.12}$$

Here again we incorporated the Hartree term to the redefinition of the impurity binding energy $\mu_i\to\tilde{\mu}_i$ and introduced the notation for the one-particle Green's-function $G_0(Q)=1/[iv_q-\xi_q]$ of a bosonic medium in the infinite-g limit. Keeping in mind the perturbative consideration in terms of the impurity-boson coupling parameter we obtain the self-energy in the simplest approximation by replacing the vertex $T(Q-K;P+K|P;Q)$ with $\tilde{g}$. The second-order calculation (see Appendix B) requires both vertex corrections that are of order $\tilde{g}^3$ and presented in Fig. 4 and the one-loop self-energy insertion which is of order $\tilde{g}^4$ and therefore is neglected in the present paper.

In general, the impurity spectrum can be found from the poles of the retarded Green's function. Particularly for the real part of the spectrum one obtains

$$\xi_i^*(p)=\xi_i(p)+\Sigma_R[\xi_i^*(p),p], \tag{2.13}$$

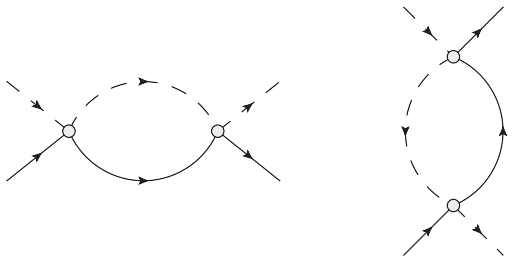

FIG. 4. One-loop diagrams contributing to the two-particle vertex $T(P;Q|Q+K;P-K)$.

where $\Sigma_R(\nu,p)=\mathrm{Re}\,\Sigma(P)|_{iv_p\to\nu+i0}$ is the real part of the analytically continued self-energy. Up to the second order of the perturbation theory Eq. (2.13) reads

$$\xi_i^*(p)=\xi_i(p)+\Sigma_R^{(1)}[\xi_i(p),p]+\Sigma_R^{(2)}[\xi_i(p),p]+\frac{1}{2}\frac{\partial}{\partial\xi_i(p)}\left\{\Sigma_R^{(1)}[\xi_i(p),p]\right\}^2, \tag{2.14}$$

where $\Sigma_R^{(1)}(\nu,p)$ and $\Sigma_R^{(2)}(\nu,p)$ are real parts of the one- and two-loop corrections to the self-energy, respectively. Absence of the Fermi surface for the impurity atom guarantees that its spectrum is gapless, i.e., $\xi_i^*(p\to0)\to0$. In the long-wavelength limit it is characterized by the effective mass only, and by expanding the right-hand side of the above equation we are in position to calculate both the impurity binding energy,

$$\mu_i=n\tilde{g}+\mu_i^{(1)}+\mu_i^{(2)}+\cdots, \tag{2.15}$$

and the inverse effective mass,

$$m_i/m_i^*=1+\Delta^{(1)}+\Delta^{(2)}+\cdots, \tag{2.16}$$

where the superscript denotes the order of perturbation theory.

III. RESULTS

A. One-loop calculations

The general low-energy structure of the impurity Green's function is visible even in the simplest approximation. Therefore it is worthwhile to discuss furthermore the first-order result in more detail that these calculations in the small-g limit can be performed analytically. In particular, for the first correction to the impurity binding energy, which is determined only by $\Sigma_R^{(1)}(-\tilde{\mu}_i,0)$, we obtained $\mu_i^{(1)}/(n\tilde{g})=\alpha\epsilon^{(1)}(\gamma)$ where the function $\epsilon^{(1)}(\gamma)$ of the mass ratio $\gamma=m/m_i$ in the case of a weakly interacting Bose gas,

$$\epsilon_{\mathrm{BEC}}^{(1)}(\gamma)=-\frac{1}{\sqrt{\gamma^2-1}}\ln\left|\frac{\gamma+\sqrt{\gamma^2-1}}{\gamma-\sqrt{\gamma^2-1}}\right|, \tag{3.1}$$

and in the TG limit,

$$\epsilon_{\mathrm{TG}}^{(1)}(\gamma)=-\int_0^1\frac{dq}{q}\ln\left|\frac{(1+q)^2+\gamma(1-q^2)}{(1-q)^2+\gamma(1-q^2)}\right| \tag{3.2}$$

is presented in Fig. 5. The dimensionless coupling constant $\alpha=\tilde{g}/(2\pi\hbar c)$ (with c being the sound velocity in both cases, i.e., $c=\sqrt{ng/m}$ and $c=\hbar p_0/m$ in BEC and TG limits, respectively) is the expansion parameter which controls the limits of applicability of our perturbative results. At finite

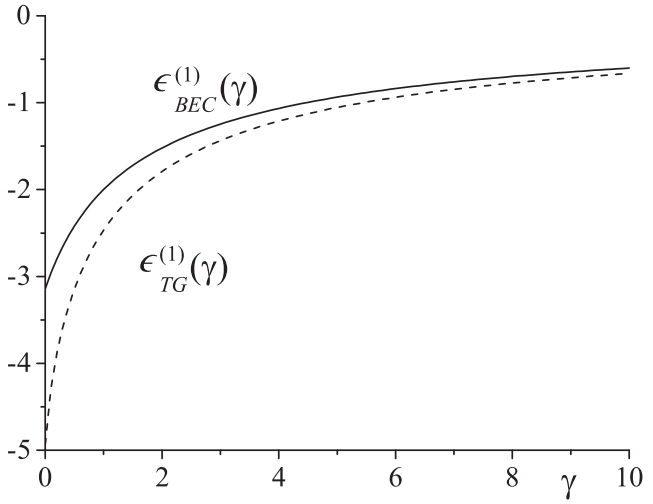

FIG. 5. Dimensionless correction $\epsilon^{(1)}(\gamma)$ to the impurity binding energy as a function of mass ratio $\gamma = m/m_i$ in the BEC (solid curve) and TG (dashed curve) limits.

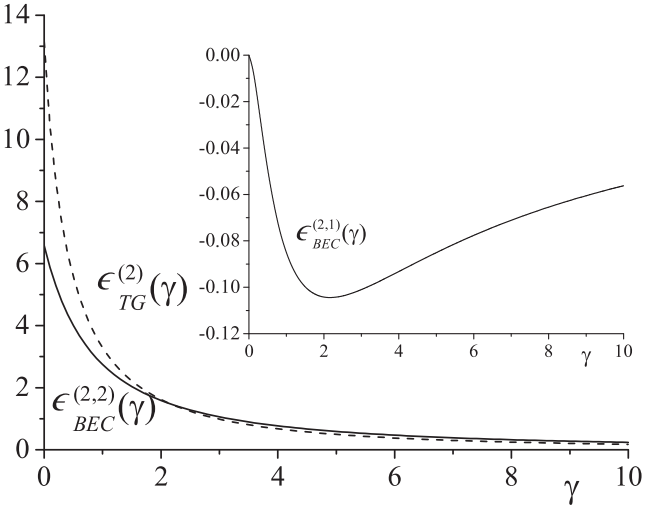

FIG. 6. The second-order binding energy corrections $\epsilon^{(2,2)}_{\rm BEC}(\gamma)$ (solid curve) and $\epsilon^{(2)}_{\rm TG}(\gamma)$ (dashed curve). The inset shows function $\epsilon^{(2,1)}_{\rm BEC}(\gamma)$.

momenta the self-energy $\Sigma^{(1)}_R[\xi_i(p),p]$ on the BEC side is a nonmonotonic function of the wave vector with logarithmic divergence at $p = m_i c/\hbar$, i.e., when the velocity of impurity reaches the value of the velocity of sound propagation in the bosonic system. Qualitatively the same behavior of the impurity self-energy is observed in the TG gas. Furthermore, from the exact solution of the Lieb and Liniger model [41] we learn that the spectrum of the system [42] contains two phononlike branches in the long-length limit for any finite value of coupling constant g. Therefore these divergences always appear indicating a nonperturbative nature of the impurity self-energy in the momentum region close to $\hbar p = m_i c$. On the other hand, it is well known that the impurity moving with supersonic velocity starts to dissipate its energy by producing elementary excitations in the bosonic bath. In the one spatial dimension this dissipation is so intensive that the imaginary part of the self-energy $\Sigma^{(1)}_I[\xi_i(p),p]/(n\tilde{g}) = -\pi\alpha/\gamma$, $(p = m_i c/\hbar + 0)$ is on the order of magnitude to the real one and in what follows we cannot neglect the damping and use Eq. (2.14) to determine the impurity spectrum at this point. But in the long-wavelength limit $p \ll m_i c/\hbar$ the damping is absent so the perturbative impurity spectrum is well defined. The one-loop contribution to the effective mass is given by $\Delta^{(1)}_{\rm TG} = -4\alpha^2$ in the TG limit and by

$$\Delta^{(1)}_{\rm BEC} = -\frac{\tilde{g}}{g}\frac{\alpha\gamma}{\gamma^2-1}\left[2\gamma - \frac{1}{\sqrt{\gamma^2-1}}\ln\left|\frac{\gamma+\sqrt{\gamma^2-1}}{\gamma-\sqrt{\gamma^2-1}}\right|\right], \tag{3.3}$$

in the dilute one-dimensional Bose gas.

No less interesting is the behavior of the impurity wave-function renormalization (quasiparticle residue) $Z_i^{-1}(p) = 1 - \partial\Sigma_R[\xi_i(p),p]/\partial\xi_i(p)$. It is easy to show by the direct calculations that the above derivative is logarithmically divergent for *any* p both in the BEC and in the TG limits. Particularly it means that the series expansion of the inverse retarded Green's function, calculated in the first order of perturbation theory, reads $[\nu \to \xi_i^*(p)]$

$$\begin{aligned}\left[G^{\rm ret}_i(\nu,p)\right]^{-1} &= \nu - \xi_i(p) - \Sigma^{(1)}_R(\nu,p)\\ &\to \nu - \xi_i^*(p) - \frac{\partial\Sigma^{(1)}_R[\xi_i^*(p),p]}{\partial\xi_i^*(p)}[\nu-\xi_i^*(p)] + \cdots\\ &\to [\nu-\xi_i^*(p)]\{1-\eta^{(1)}(p)\ln[\nu-\xi_i^*(p)] + \cdots\},\end{aligned} \tag{3.4}$$

where the ellipses stand for the finite terms. Being independent of the wave vector these divergences suggest the *exact* Green's function has a branch-point singularity $[\eta(0) = \eta]$,

$$G^{\rm ret}_i(\nu, p\to 0)|_{\nu\to\xi_i^*(p)} \propto \frac{1}{[\nu-\xi_i^*(p)]^{1-\eta}}. \tag{3.5}$$

This statement is supported by the explicit calculation of the exponent η since in both analytically available cases we obtained the same value,

$$\eta^{(1)}_{\rm BEC} = \eta^{(1)}_{\rm TG} = n\tilde{g}^2/(2\pi\hbar m c^3), \tag{3.6}$$

on the one-loop level. Looking ahead it should be noted that this power-law behavior of the impurity Green's function is confirmed perfectly by the second-order perturbation theory calculations.

B. Two-loop results

The numerical calculations up to the second order of perturbation theory requires more computational effort. Particularly the expansion for the binding energy correction in the BEC limit reads $\mu_i^{(2)}/n\tilde{g} = \frac{\tilde{g}}{g}\alpha^2\epsilon^{(2,1)}_{\rm BEC}(\gamma) + \alpha^2\epsilon^{(2,2)}_{\rm BEC}(\gamma)$. In the TG case the above expansion contains the single term $\mu_i^{(2)}/(n\tilde{g}) = \alpha^2\epsilon^{(2)}_{\rm TG}(\gamma)$. For comparison in Fig. 6 we built all three curves. It is seen that function $\epsilon^{(2,2)}_{\rm BEC}(\gamma)$ is almost two orders of magnitude larger than $\epsilon^{(2,2)}_{\rm BEC}(\gamma)$, which particularly means that, even in a weakly interacting Bose gas, the quasiparticle-mediated impurity potential is not negligible. In the

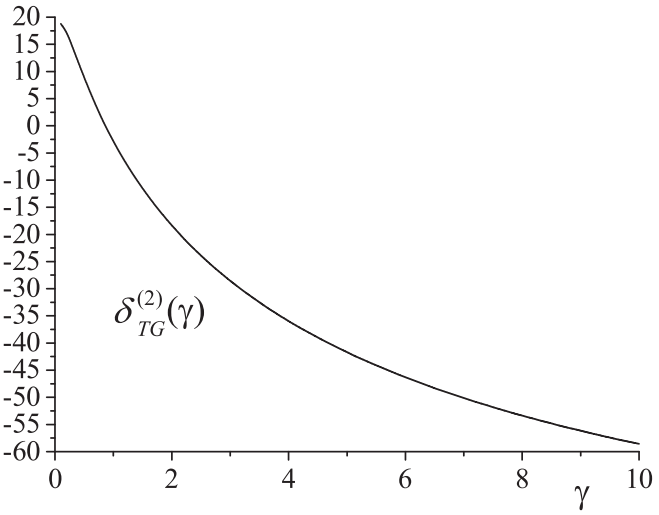

FIG. 7. Function $\delta^{(2)}_{\rm TG}(\gamma)$ determining the two-loop result for an effective mass in the TG limit.

TG limit when $\gamma = 1$ our results for the impurity binding energy $\mu_i|_{\gamma=1} = n\tilde{g}(1 - \frac{\pi^2}{4}\alpha + \frac{\pi^2}{3}\alpha^2 + \cdots)$ exactly reproduce the first three terms of an analytical formula [30] obtained within the Bethe ansatz wave function. The similar expansions were derived for the second-order corrections to the particle effective mass in the BEC $\Delta^{(2)}_{\rm BEC} = (\tilde{g}/g)^2\alpha^2\delta^{(2,1)}_{\rm BEC}(\gamma) + (\tilde{g}/g)\alpha^2\delta^{(2,2)}_{\rm BEC}(\gamma)$ and TG $\Delta^{(2)}_{\rm TG} = \alpha^3\delta^{(2)}_{\rm TG}(\gamma)$ limits, respectively [functions $\delta^{(2,1)}_{\rm BEC}(\gamma)$, $\delta^{(2,2)}_{\rm BEC}(\gamma)$, and $\delta^{(2)}_{\rm TG}(\gamma)$ are plotted in Figs. 7 and 8].

It is easy to verify that the numerically calculated TG effective mass in the integrable limit perfectly coincides with the exact expansion $m_i/m_i^*|_{\gamma=1} = 1 - 4\alpha^2 + 4(\pi^2/3 - 4)\alpha^3 + \cdots$. Figure 7 reveals the strong dependence of function $\delta^{(2)}_{\rm TG}(\gamma)$ on the mass ratio parameter γ. This signals the breakdown of an ordinary perturbation theory at large mass imbalance in the TG limit, and in order to resolve this problem one needs to take into account an infinite series of diagrams

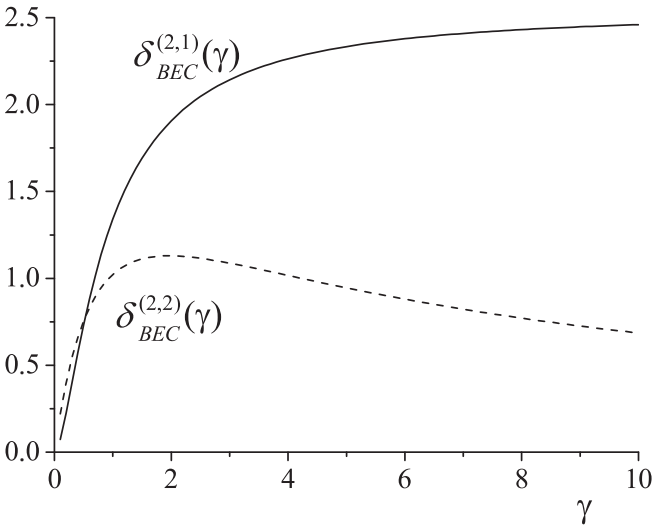

FIG. 8. Dimensional functions $\delta^{(2,1)}_{\rm BEC}(\gamma)$ (solid curve) and $\delta^{(2,2)}_{\rm BEC}(\gamma)$ (dashed curve).

(ladder summation in the particle-particle or particle-hole [43] channels).

Our second-order perturbative calculations of the self-energy allow for obtaining the above-presented exponent η on the two-loop level. In the same manner as was performed before [see Eq. (3.4)] by the explicit series expansion of the retarded impurity Green's function in the vicinity of a singular point $\nu \to \xi_i^*(p)$ we have

$$\left[G_i^{\rm ret}(\nu,p)\right]^{-1} = [\nu - \xi_i^*(p)]\{1 - [\eta^{(1)} + \eta^{(2)}]\ln[\nu - \xi_i^*(p)] + \tfrac{1}{2}[\eta^{(1)}]^2\ln^2[\nu - \xi_i^*(p)] \pm \cdots\},$$

where $\eta^{(1)}$ already was given by Eq. (3.6) and the value of the second correction $\eta^{(2)}$ depends strongly on the properties of the bosonic environment. The presence of the $\ln^2$ divergences with a proper factor $\frac{1}{2}[\eta^{(1)}]^2$ proves our original suggestion (3..5). Combining the first- and second-order results we obtain in the BEC limit,

$$\eta^{(1)}_{\rm BEC} + \eta^{(2)}_{\rm BEC} = \frac{n\tilde{g}^2}{2\pi\hbar mc^3} \times \left[1 - \frac{\alpha}{2\sqrt{\gamma^2-1}}\ln\left|\frac{\gamma+\sqrt{\gamma^2-1}}{\gamma-\sqrt{\gamma^2-1}}\right|\right]^2. \tag{3.7}$$

The TG limit demonstrates an unexpected behavior $\eta^{(2)}_{\rm TG} = 0$ instead. Such a dependence of the second-order correction $\eta^{(2)}$ led us to the conclusion that the exact value of an exponent responsible for the nonanalytic behavior of the impurity Green's function is given by $\eta = n(\partial\mu_i/\partial n)^2/(2\pi\hbar mc^3)$. Indeed, it is easy to verify that $\mu_i^{(1)}$, that determines $\eta^{(2)}$, does not depend on the density of the medium in the TG limit and that a derivative $\partial\mu_i^{(1)}/\partial(n\tilde{g})$ on the BEC side is equal to the expression in the square brackets of Eq. (3.7). Of course, it is too optimistic to write down the whole result only with the second-order perturbative calculations at hand, but exactly the same formula for η as well as a singular behavior (3.5) of the impurity propagator can be proven by using a technique similar to that of Refs. [44,45].

IV. CONCLUSIONS

To summarize, by applying perturbation theory up to the second order we have revealed the detailed low-energy structure of the spectrum (binding energy and effective mass) for a mobile impurity immersed in the one-dimensional bosonic environment. Considering our system as a Fermi-Bose mixture with the vanishingly small fermionic density we found that the interaction with a bosonic medium crucially changes the single-particle impurity Green's function providing the latter exhibits branch-point singularity. Using our second-order perturbative results we have proposed the general formula for the nonuniversal exponent determining this behavior. It also is demonstrated that the induced interaction, especially in the case of a large mass imbalance, has a profound effect on the behavior of a single impurity atom in the one-dimensional Bose gas.

ACKNOWLEDGMENTS

Stimulating discussions with Professor I. Vakarchuk and Dr. A. Rovenchak are gratefully acknowledged. This work was supported partly by Project FF-30F (Project No. 0116U001539) from the Ministry of Education and Science of Ukraine.

APPENDIX A: BEC LIMIT

The calculations of the one-loop diagrams (see Fig. 1) on the BEC side at zero temperature yield

$$\Sigma^{(1)}(P) = -\frac{1}{L}\sum_{k\neq 0}\frac{n\tilde{g}^2}{\alpha_k}\frac{1}{E_k + \xi_i(k+p) - i\nu_p}. \tag{A1}$$

The second-order result is more cumbersome for evaluation nevertheless still tractable. While calculating the one-loop correction to vertices we find that only four diagrams in Fig. 2 are nonzero at $T = 0$. Furthermore, by substituting these eight terms in Eq. (2.10) one concludes that only five contribute to the self-energy with the result,

$$\begin{aligned}\Sigma^{(2)}(P) = &-\frac{1}{2L^2}\sum_{k,s\neq 0}\frac{n^2\tilde{g}^4}{\alpha_k\alpha_s}\frac{1}{E_s + E_k + \xi_i(s+k+p) - i\nu_p}\left[\frac{1}{E_k + \xi_i(k+p) - i\nu_p} + \frac{1}{E_s + \xi_i(s+p) - i\nu_p}\right]^2\\
&+\frac{1}{L^2}\sum_{k,s\neq 0}\frac{n\tilde{g}^3}{\alpha_k\alpha_s\alpha_{k+s}}\frac{1}{E_s + \xi_i(s-p) - i\nu_p}\frac{1}{E_k + \xi_i(k+p) - i\nu_p}\\
&-\frac{1}{2L^2}\sum_{k,s\neq 0}\frac{n\tilde{g}^3}{\alpha_k\alpha_s\alpha_{k+s}}\frac{1}{E_k + E_s + \xi_i(k+s+p) - i\nu_p}\left[\frac{D_+(k,s)}{E_{k+s} + \xi_i(s+k+p) - i\nu_p} - \frac{D_-(k,s)}{E_k + E_s + E_{k+s}}\right]\\
&\times\left[\frac{1}{E_k + \xi_i(k+p) - i\nu_p} + \frac{1}{E_s + \xi_i(s+p) - i\nu_p}\right],\end{aligned} \tag{A2}$$

where the symmetric functions $D_\pm(k,s)$ read

$$D_\pm(k,s) = \frac{\hbar^2}{2m}[k(k+s)(\alpha_k - 1)(\alpha_{k+s} \pm 1) + s(s+k)(\alpha_s - 1)(\alpha_{k+s} \pm 1) \pm ks(\alpha_k - 1)(\alpha_s - 1)].$$

APPENDIX B: TG GAS

The self-energy calculations in the TG limit are much simpler. For instance, on the one-loop level we obtained

$$\Sigma^{(1)}(P) = \frac{1}{L}\sum_q \tilde{g}^2(1 - n_q)\Pi_q(P) = -\frac{1}{L}\sum_q \tilde{g}^2 n_q t_q(P), \tag{B1}$$

where $n_q = \theta(p_0 - |q|)$ is a unit step function. The impurity-boson particle-hole diagram reads

$$\Pi_q(P) = \frac{1}{L}\sum_k \frac{n_k}{i\nu_p - \xi_q + \xi_k - \xi_i(k - q + p)}, \tag{B2}$$

and the notation for the particle-particle bubble,

$$t_q(P) = \frac{1}{L}\sum_k \frac{1 - n_k}{\xi_k + \xi_i(k + q + p) - \xi_q - i\nu_p} \tag{B3}$$

is used. Taking into account the vertex corrections (see Fig. 4) the calculations in the next order of perturbation theory give

$$\Sigma^{(2)}(P) = \frac{1}{L}\sum_q \tilde{g}^3 n_q t_q^2(P) - \frac{1}{L}\sum_q \tilde{g}^3(1 - n_q)\Pi_q^2(P). \tag{B4}$$

Both $\Pi_q(P)$ and $t_q(P)$ on the "mass-shell" $i\nu_p \to \xi_i(p)$ can be written in terms of elementary functions.

[1] A. Novikov and M. Ovchinnikov, J. Phys. A: Math. Theor. **42**, 135301 (2009).

[2] A. Novikov and M. Ovchinnikov, J. Phys. B **43**, 105301 (2010).

[3] S. P. Rath and R. Schmidt, Phys. Rev. A **88**, 053632 (2013).

[4] W. Li and S. Das Sarma, Phys. Rev. A **90**, 013618 (2014).

[5] J. Levinsen, M. M. Parish, and G. M. Bruun, Phys. Rev. Lett. **115**, 125302 (2015).

[6] R. S. Christensen, J. Levinsen, and G. M. Bruun, Phys. Rev. Lett. **115**, 160401 (2015).

[7] F. Grusdt, Y. E. Shchadilova, A. N. Rubtsov, and E. Demler, Sci. Rep. **5**, 12124 (2015).
[8] J. V. W. Casteels, K. Van Houcke, J. Tempere, J. Ryckebusch, and J. T. Devreese, New J. Phys. **17**, 033023 (2015).
[9] L. A. Peña Ardila and S. Giorgini, Phys. Rev. A **92**, 033612 (2015).
[10] L. A. Peña Ardila and S. Giorgini, Phys. Rev. A **94**, 063640 (2016).
[11] B. Kain and H. Y. Ling, Phys. Rev. A **94**, 013621 (2016).
[12] A. Lampo, S. H. Lim, M. A. Garcia-March, and M. Lewenstein, Quantum **1**, 30 (2017).
[13] E. Krotscheck, M. Saarela, K. Schorkhuber, and R. Zillich, Phys. Rev. Lett. **80**, 4709 (1998).
[14] J. Boronat and J. Casulleras, Phys. Rev. B **59**, 8844 (1999).
[15] D. E. Galli, G. L. Masserini, and L. Reatto, Phys. Rev. B **60**, 3476 (1999).
[16] G. Panochko, V. Pastukhov, and I. Vakarchuk, arXiv:1706.07768.
[17] M. G. Hu, M. J. Van de Graaff, D. Kedar, J. P. Corson, E. A. Cornell, and D. S. Jin, Phys. Rev. Lett. **117**, 055301 (2016).
[18] N. B. Jorgensen, L. Wacker, K. T. Skalmstang, M. M. Parish, J. Levinsen, R. S. Christensen, G. M. Bruun, and J. J. Arlt, Phys. Rev. Lett. **117**, 055302 (2016).
[19] A. O. Caldeira and A. H. Castro Neto, Phys. Rev. B **52**, 4198 (1995).
[20] A. H. Castro Neto and M. P. A. Fisher, Phys. Rev. B **53**, 9713 (1996).
[21] D. M. Gangardt and A. Kamenev, Phys. Rev. Lett. **102**, 070402 (2009).
[22] M. Ovchinnikov and A. Novikov, J. Chem. Phys. **132**, 214101 (2010).
[23] K. A. Matveev and A. V. Andreev, Phys. Rev. B **86**, 045136 (2012).
[24] E. Burovski, V. Cheianov, O. Gamayun, and O. Lychkovskiy, Phys. Rev. A **89**, 041601(R) (2014).
[25] A. S. Dehkharghani, A. G. Volosniev, and N. T. Zinner, Phys. Rev. A **92**, 031601(R) (2015).
[26] A. Petkovic and Z. Ristivojevic, Phys. Rev. Lett. **117**, 105301 (2016).
[27] M. A. Cazalilla, R. Citro, T. Giamarchi, E. Orignac, and M. Rigol, Rev. Mod. Phys. **83**, 1405 (2011).
[28] A. Imambekov, T. L. Schmidt, and L. I. Glazman, Rev. Mod. Phys. **84**, 1253 (2012).
[29] A. G. Volosniev and H.-W. Hammer, Phys. Rev. A **96**, 031601(R) (2017).
[30] J. B. McGuire, J. Math. Phys. **6**, 432 (1965).
[31] J. B. McGuire, J. Math. Phys. **7**, 123 (1966).
[32] H. Castella and X. Zotos, Phys. Rev. B **47**, 16186 (1993).
[33] O. Gamayun, A. G. Pronko, and M. B. Zvonarev, Nucl. Phys. B **892**, 83 (2015).
[34] O. Gamayun, A. G. Pronko, and M. B. Zvonarev, New J. Phys. **18**, 045005 (2016).
[35] J. Catani, G. Lamporesi, D. Naik, M. Gring, M. Inguscio, F. Minardi, A. Kantian, and T. Giamarchi, Phys. Rev. A **85**, 023623 (2012).
[36] L. Parisi and S. Giorgini, Phys. Rev. A **95**, 023619 (2017).
[37] F. Grusdt, G. E. Astrakharchik, and E. A. Demler, arXiv:1704.02606.
[38] C. Mora and Y. Castin, Phys. Rev. A **67**, 053615 (2003).
[39] V. Pastukhov, J. Low Temp. Phys. **186**, 148 (2017).
[40] A. A. Abrikosov, L. P. Gor'kov, and I. Y. Dzyaloshinskii, *Quantum Field Theoretical Methods In Statistical Physics* (Pergamon, Oxford, 1965).
[41] E. H. Lieb and W. Liniger, Phys. Rev. **130**, 1605 (1963).
[42] E. H. Lieb, Phys. Rev. **130**, 1616 (1963).
[43] O. Gamayun, Phys. Rev. A **89**, 063627 (2014).
[44] V. Pastukhov, J. Phys. A: Math. Theor. **48**, 405002 (2015).
[45] V. Pastukhov, Ann. Phys. (NY) **372**, 149 (2016).